

## Interband Optical Absorption and Electronic $s$ - $d$ Transition in Rb and Cs at High Pressures

H. Tups, K. Takemura, and K. Syassen

*Physikalisches Institut III, Universität Düsseldorf, D-4000 Düsseldorf 1, Federal Republic of Germany*

(Received 13 September 1982)

The effect of pressure on the optical properties of Rb and Cs is studied by reflection spectroscopy. Under pressure, both metals exhibit a strong increase of the interband absorption with prominent structure below 3 eV. The strength of the absorption is intimately related to a transfer of conduction electrons from  $s$ - into  $d$ -like states. The optical properties provide conclusive evidence that the pressure-induced bcc-fcc transition in both metals occurs at the same critical value of  $d$ -band occupancy.

PACS numbers: 78.40.Kc, 64.70.Kb

The pressure-induced occupation of  $d$ -like states at the expense of  $sp$  states is a common phenomenon in metals with partly occupied or empty  $d$  shells. The  $s$ - $d$  transfer plays an important role in recent theoretical attempts to explain or predict the systematics of high-pressure structural phase transformations.<sup>1</sup> We report on the first *spectroscopic* investigation of the pressure-induced  $s$ - $d$  transfer and related structural transitions in metals using optical reflection spectroscopy.

The prototype example for an  $s$ - $d$  transition appears to be the behavior of Cs in the moderate pressure range 0–50 kbar. The unusually high compressibility and an isostructural volume collapse by 9% at 42 kbar have been attributed to the occupation of  $d$ -like states.<sup>2-4</sup> We find that the onset of the  $6s \rightarrow 5d$  transition in Cs is responsible for a dramatic increase of the optical interband absorption in comparison to the optical properties at ordinary pressure.<sup>5</sup> In a similar optical study we have investigated the pressure-induced  $5s \rightarrow 4d$  electronic transition in Rb. A comparison of the high-pressure optical properties of Cs and Rb reveals a close relationship between interband absorption strength, degree of  $s$ - $d$  transfer, and structural bcc-fcc transition, which occurs at 23 kbar in Cs (Ref. 6) and 70 kbar (Ref. 7) in Rb.

The reflectivities of Rb and Cs were measured for photon energies  $0.5 \text{ eV} < \hbar\omega < 3.5 \text{ eV}$  with a gasketed diamond-anvil cell and a micro-optical spectrophotometric system.<sup>8</sup> Samples of 99.93% purity were loaded into the cylindrical gasket hole (0.2 mm diam and 0.13 mm height) under argon atmosphere. No pressure medium was used. The reflectivity was measured from spots of roughly  $35 \mu\text{m}$  diam at the interface between diamond window and sample. Pressures were determined by the ruby fluorescence method.

Reflection spectra of Cs and Rb in their bcc

(phase I) and fcc (phase II) crystal structures are shown in Fig. 1. A comparison of reflection spectra at the lowest pressures with those at ordinary conditions<sup>5</sup> yields already small pressure effects. In Cs-I a drastic continuous change of the reflectivity occurs on raising the pressure to 19 kbar. A steep edge develops in the near-infrared (ir) with a minimum in reflectivity at 1.2 eV. At the bcc-fcc phase boundary the reflection spectrum changes abruptly. In Cs-II (23–42 kbar) the ir reflectivity edge is extended over a slightly

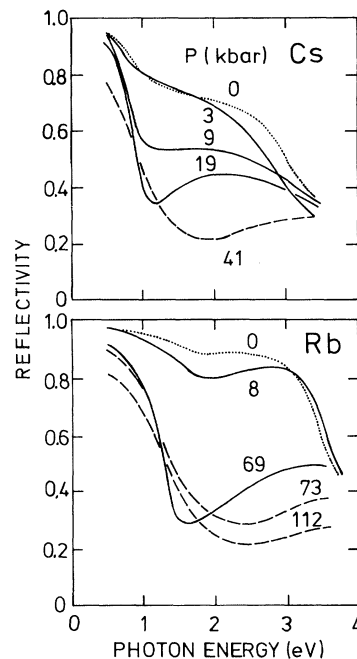


FIG. 1. Optical reflectivity of Cs and Rb at several pressures in the bcc phase (solid lines) and the fcc phase (dashed lines). The reflectivity is measured at the diamond-sample interface. The dotted lines correspond to reflection spectra at 1 bar calculated from the dielectric constants given in Ref. 5.

larger photon energy range and the reflectivity minimum is shifted to higher energies compared to Cs-I at 19 kbar. A strikingly similar optical behavior is found for Rb-I and Rb-II (stable from 70 to 128 kbar<sup>7</sup>). The main difference between Cs and Rb is a 0.3-eV shift of the reflectivity edge to higher energy. All pressure-induced changes of the optical properties are reversible. Uncertainties in the absolute values of the reflectivities are estimated to be  $\pm 0.03$ .

Figure 2 shows the real part  $\sigma(\omega)$  of the optical conductivity of Cs at several pressures.  $\sigma(\omega)$  is derived from the reflection spectra by a Kramers-Kronig (KK) analysis.<sup>9</sup> Below 0.5 eV some  $\sigma(\omega)$  spectra are extrapolated by a Drude-type behavior with band mass assumed equal to optical mass  $m^*$  and scattering time estimated from the pressure dependence of the dc resistivity.<sup>10</sup> Similar results were obtained for  $\sigma(\omega)$  of Rb. The volume dependence of the effective number of electrons  $n_{\text{eff}}$ <sup>9</sup> contributing to the non-Drude-type absorption (also shown in Fig. 2) reflects the continuous increase of the integrated interband conductivity  $\sigma_{\text{ib}}$ , which in Rb starts at a smaller relative volume compared to Cs.

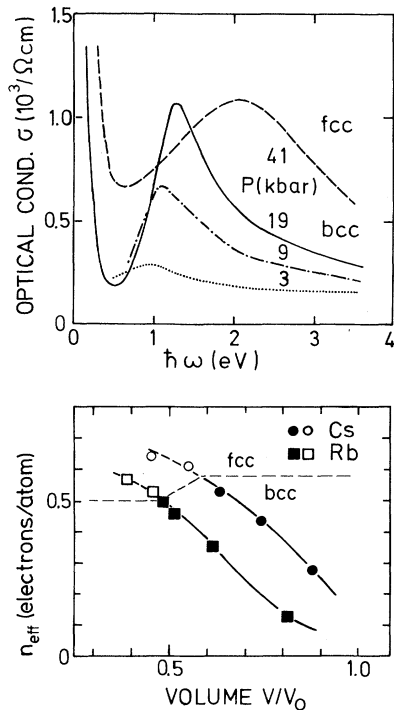


FIG. 2. (Top) Real part  $\sigma(\omega)$  of the optical conductivity of Cs at high pressure and (bottom) volume dependence of the effective number  $n_{\text{eff}}$  of electrons per atom contributing to interband absorption in Cs and Rb.

Our interpretation of the pressure-induced optical absorption in Cs and Rb is entirely based on interband transitions between one-electron energy levels. We rule out surface-plasmon excitations, because reflectivity measurements for Ag and Na at high pressure do not provide any indication for unusual absorption features in the spectral range 0.5–4.0 eV. Charge-density waves, which have been invoked in the discussion of optical-absorption features of K,<sup>11</sup> will not be considered.

Figure 3 shows the relevant part of the band structure of bcc Cs at two different volumes.<sup>12</sup> The interband absorption threshold in Cs at normal pressure [ see Fig. 3(a) ] deviates from the prediction of the nearly free electron (NFE) model (Wilson-Butcher theory).<sup>5</sup> This deviation has been explained by the existence of empty  $d$ -like states close to the Fermi level. Under pressure, the NFE-like  $6s$  band of Cs-I is progressively distorted at the Brillouin-zone (BZ) boundary because of the increased energetic overlap and hybridization with the lowest  $5d$  subband<sup>12</sup> [ see Fig. 3(b) ]. When the first band moves below the Fermi level at  $N_1$ , a large joint density of states (parallel band effect) evolves between occupied states near  $N_1$  and excited states near  $N_1'$  ( $p$  symmetry) and  $N_2$  ( $d$  symmetry). According to dipole selection rules interband transitions into both excited bands are allowed in the vicinity of the  $N$  point but not exactly at  $N$ . The  $N_1$ - $N_2$  splitting remains essentially constant at reduced volume. The increase of the  $N_1$ - $N_1'$  splitting accounts for the slight shift of the peak in  $\sigma(\omega)$  to higher energy (see Fig. 2).

In fcc Cs there is a very similar situation, i.e., because of the admixture of  $d$  character, the lowest conduction band is distorted at the BZ boundary near the  $X$  and  $L$  points.<sup>3,13</sup> An absorp-

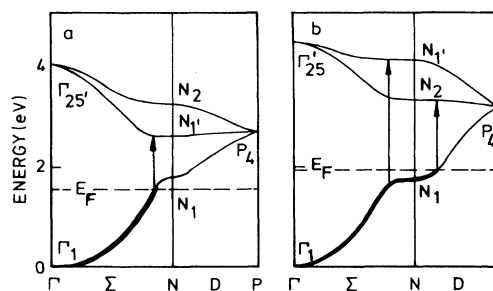


FIG. 3. Characteristic features of the energy-band structure of bcc Cs near the Fermi level for relative volumes (a)  $V/V_0 = 1$  and (b)  $V/V_0 = 0.64$  ( $P \approx 18$  kbar), according to Ref. 12. The energy scale is approximate.

tion threshold is located near the  $X$  point with an energy close to the  $X_1$ - $X_3$  splitting of roughly 0.7 eV. We tentatively assign the maximum in  $\sigma(\omega)$  at 2 eV to transitions between bands near the  $L$  point, where the  $L_1$ - $L_2'$  and the  $L_1$ - $L_3$  splittings are close to 2 eV.<sup>13</sup>

The qualitative interpretation of reflection spectra and optical conductivity of Rb would be almost identical to the above discussion for Cs. The main difference arises from systematic trends in the splitting of corresponding states on going from Cs towards the lighter alkali metals.<sup>12</sup>

The reflection spectra of Cs-I at 19 kbar and Rb-I at 69 kbar (see Fig. 1) suggest that the strength of the interband absorption is similar in both metals just before the bcc-fcc transition. A more quantitative result is obtained from a comparison of the  $n_{\text{eff}}$  values (Fig. 2). At the bcc-fcc transition  $n_{\text{eff}}$  is 0.58 for Cs and 0.50 for Rb. We now assume that transition matrix elements between corresponding states in Rb and Cs are identical and, furthermore, we take into account that the characteristic absorption features in Rb are shifted by 0.3 eV to higher energy compared to Cs. From the relation between  $n_{\text{eff}}$  and the joint density of states per atom  $J(\omega)$ ,<sup>9</sup> it then follows that the integrated  $J(\omega)$  is very similar in Rb and Cs at the bcc-fcc transition. Since in first approximation  $J(\omega)$  is proportional to the amount of  $d$  character below the Fermi level, we arrive at the conclusion that the phase transition occurs at a critical value of  $d$ -band occupancy, which is almost identical in Rb and Cs.

The isostructural volume collapse of Cs at 42 kbar is believed to be related to the occupation of a second pocket of  $d$  states at the  $X$  point (Lifshitz transition) and to a negative contribution of thermal lattice vibrations to the total pressure.<sup>4, 14</sup> As shown in Fig. 4, the ir reflectivity drops abruptly at the II-III transition. Since at this transition the resistivity increases by a factor of 2.4,<sup>10</sup> we attribute the low ir reflectivity primarily to free-carrier (Drude-type) absorption, which dominates over possible low-lying ( $\hbar\omega < 1$  eV) interband transitions (see fcc band structures in Ref. 13). Qualitatively, the discontinuity of the Drude-type absorption is explained by the transition to a two-band situation with a highly anisotropic large Fermi surface<sup>13</sup> and an associated increase of the intraband and interband electron scattering rate. At 300 K electron-phonon scattering is expected to be particularly efficient because of the low melting ( $T_m \sim 360$  K) and Debye ( $\theta_D \lesssim 100$  K) temperature. Furthermore, phonon-

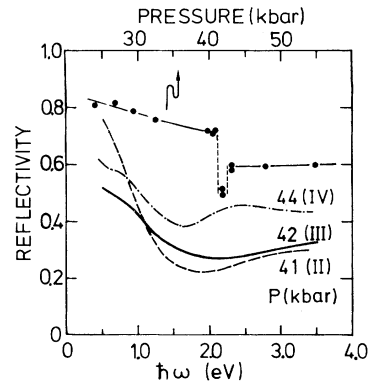


FIG. 4. Optical reflectivity of phases II, III, and IV of Cs between 41 and 44 kbar and pressure scan of the reflectivity at 0.6 eV.

disorder-induced broadening of the electronic states may contribute significantly to the electron-phonon coupling on both sides of the transition.<sup>14</sup> Similar arguments partly account for the continuous decrease of the ir reflectivity of Cs-II (see Fig. 4).

At 42.5 kbar Cs transforms to a tetragonal phase Cs-IV.<sup>15</sup> From visual observation, Cs-IV is optically anisotropic. The unpolarized reflection spectrum of Cs-IV at 44 kbar (see Fig. 4) is an average over different crystalline orientations. Again, the low ir reflectivity is indicative of the two-band nature of the Fermi-surface topology. While the resistivities of Cs-II at 41 kbar and Cs-IV at 44 kbar are identical,<sup>10</sup> the ir reflectivities differ by a substantial amount. We presume that low-lying interband transitions contribute significantly to the optical absorption of Cs-IV in the ir spectral range. In other words, a large density of occupied and unoccupied states near the Fermi energy should be a characteristic feature of the band structure of Cs-IV at 44 kbar.

In summary, the pressure-induced optical absorption in Cs is the first spectroscopic manifestation of the increased  $d$  character of the conduction electrons. The optical absorption of Rb in the 120-kbar range clearly shows that the  $5s \rightarrow 4d$  transition proceeds in a way very similar to the  $6s \rightarrow 5d$  transition in Cs below 42 kbar. The volume dependence of the integrated interband optical conductivity in the bcc and fcc phases of both metals provides conclusive experimental evidence for the strong correlation between  $d$ -band occupancy and crystal structure stability. Further optical investigations of Na and the predicted  $s$ - $d$  transition in K (Ref. 16) will be reported together with a more complete report of

the present work.

We thank Professor A. Otto for his continuous interest. This work was supported in part by the Alexander von Humboldt-Stiftung.

<sup>1</sup>J. C. Duthie and D. G. Pettifor, *Phys. Rev. Lett.* **38**, 564 (1977); J. A. Moriarty and A. K. McMahan, *Phys. Rev. Lett.* **48**, 809 (1982); H. L. Skriver, private communication.

<sup>2</sup>D. B. McWhan, G. Parisot, and D. Bloch, *J. Phys. F* **4**, L69 (1974).

<sup>3</sup>A. K. McMahan, *Phys. Rev. B* **17**, 1521 (1978).

<sup>4</sup>D. Glötzel and A. K. McMahan, *Phys. Rev. B* **20**, 3210 (1979).

<sup>5</sup>N. V. Smith, *Phys. Rev. B* **2**, 2840 (1970).

<sup>6</sup>H. T. Hall, L. Merrill, and J. D. Barnett, *Science* **146**, 1297 (1964).

<sup>7</sup>K. Takemura and K. Syassen, to be published.

<sup>8</sup>K. Syassen and R. Sonnenschein, *Rev. Sci. Instrum.* **53**, 644 (1982), and references therein.

<sup>9</sup>The KK analysis was performed such that  $m^*$  determined from the sum rule for  $\sigma_{\text{ib}}$  and from the Cohen plot of the real part of the dielectric function (see Ref. 5) are consistent. The effective number of electrons  $n_{\text{eff}}$  contributing to  $\sigma_{\text{ib}}$  above 3.5 eV is roughly 35%

of  $n_{\text{eff}}$  corresponding to  $0.5 < \hbar\omega < 3.5$  eV. Uncertainties of absolute values of  $\sigma(\omega)$  are estimated to be  $\pm 10\%$ . Relations between optical terms used throughout the text are

$$N^{-1} \int_0^\infty \sigma_{\text{ib}}(\omega) d\omega \propto (m^* - m_0)/m^* = n_{\text{eff}} \\ \propto \int_0^\infty [M(\omega) \cdot J(\omega)/\omega] d\omega$$

[ $N$  = atom and conduction-electron density,  $M(\omega)$  = average value of squared transition matrix elements].

<sup>10</sup>D. B. McWhan and A. L. Stevens, *Solid State Commun.* **7**, 301 (1969). New resistance measurements for Rb are reported by K. Ullrich, thesis, Universität Köln, 1979 (unpublished).

<sup>11</sup>A. W. Overhauser, *Adv. Phys.* **27**, 343 (1978), and references therein.

<sup>12</sup>F. S. Ham, *Phys. Rev.* **128**, 82, 2524 (1962); see also J. P. Jan, A. H. McDonald, and H. L. Skriver, *Phys. Rev. B* **21**, 5584 (1980).

<sup>13</sup>J. Yamashita and S. Asano, *J. Phys. Soc. Jpn.* **29**, 264 (1970); S. G. Louie and M. L. Cohen, *Phys. Rev. B* **10**, 3237 (1974).

<sup>14</sup>L. Dagens and C. Lopez-Rios, *J. Phys. F* **9**, 2195 (1979).

<sup>15</sup>K. Takemura, S. Minomura, and O. Shimomura, preceding Letter [*Phys. Rev. Lett.* **49**, 1772 (1982)].

<sup>16</sup>M. S. T. Bukowinski, in *High Pressure Science and Technology*, edited by K. D. Timmerhaus and M. S. Barber (Plenum, New York, 1979), Vol. 2, p. 237.

## Polarized Low-Energy Positrons: A New Probe of Surface Magnetism

D. W. Gidley and A. R. Köymen

*Physics Department, University of Michigan, Ann Arbor, Michigan 48109*

and

T. Weston Capehart

*Physics Department, General Motors Research Laboratories, Warren, Michigan 48090*

(Received 27 September 1982)

A polarized beam of low-energy positrons has been used for the first time as a probe of surface magnetism. The polarization,  $P_e^-$ , of electrons captured at a Ni(110) surface to form positronium is measured. The temperature dependence of  $P_e^-$ , fitted by a power law, yields an exponent of  $\beta_1 = 0.7 \pm 0.1$ , in qualitative agreement with calculations of the critical exponent for the surface-layer magnetization. Rapid quenching of the ferromagnetic order is observed for submonolayer coverages of oxygen.

PACS numbers: 75.25.+z, 73.20.Cw, 78.70.Bj

The investigation of surface magnetism has recently become a topic of active theoretical and experimental interest. Calculations<sup>1-5</sup> of surface electronic properties of the ferromagnetic transition metals, performed with a thin slab geometry, predict band structure, charge and net spin densities, surface states, etc. The experimental

techniques now being developed to study surface magnetic properties include polarized photoemission<sup>6</sup> and field emission,<sup>7</sup> electron capture by ions in glancing collisions,<sup>8</sup> polarized low-energy electron scattering,<sup>9</sup> neutron reflection,<sup>10</sup> and ferromagnetic resonance absorption.<sup>11</sup> Experimental tests are limited by the requirement that